Michigan Technological University
Digital Commons @ Michigan Tech

Department of Physics Publications
Department of Physics

10-29-2009

In situ probing of electromechanical properties of an individual ZnO nanobelt

Anjana Asthana
Michigan Technological University

Kasra Momeni
Michigan Technological University

Abhishek Prasad
Michigan Technological University

Yoke Khin Yap
Michigan Technological University

Reza Shahbazian Yassar
Michigan Technological University

Follow this and additional works at: https://digitalcommons.mtu.edu/physics-fp

Recommended Citation

Asthana, A., Momeni, K., Prasad, A., Yap, Y. K., & Yassar, R. S. (2009). In situ probing of electromechanical properties of an individual ZnO nanobelt. *Applied Physics Letters, 95*, 172106. http://dx.doi.org/10.1063/1.3241075
Retrieved from: https://digitalcommons.mtu.edu/physics-fp/299

Follow this and additional works at: https://digitalcommons.mtu.edu/physics-fp

Applied Physics Letters

In situ probing of electromechanical properties of an individual ZnO nanobelt

Cite as: Appl. Phys. Lett. **95**, 172106 (2009); https://doi.org/10.1063/1.3241075
Submitted: 12 August 2009 . Accepted: 01 September 2009 . Published Online: 29 October 2009

Anjana Asthana, Kasra Momeni, Abhishek Prasad, Yoke Khin Yap, and Reza Shahbazian Yassar

View Online

Export Citation

ARTICLES YOU MAY BE INTERESTED IN

In situ probing electrical response on bending of ZnO nanowires inside transmission electron microscope
Applied Physics Letters **92**, 213105 (2008); https://doi.org/10.1063/1.2936080

In situ probing mechanical properties of individual tungsten oxide nanowires directly grown on tungsten tips inside transmission electron microscope
Applied Physics Letters **89**, 221908 (2006); https://doi.org/10.1063/1.2397547

Very low Schottky barrier height at carbon nanotube and silicon carbide interface
Applied Physics Letters **106**, 123501 (2015); https://doi.org/10.1063/1.4916248

Lock-in Amplifiers up to 600 MHz
starting at
$6,210

Zurich Instruments
Watch the Video

AIP Publishing

© 2009 American Institute of Physics.

In situ probing of electromechanical properties of an individual ZnO nanobelt

Anjana Asthana,[1,a)] Kasra Momeni,[1] Abhishek Prasad,[2] Yoke Khin Yap,[2,a)] and Reza Shahbazian Yassar[1,a)]
[1]*Department of Mechanical Engineering-Engineering Mechanics, Michigan Technological University, Houghton, Michigan 49931, USA*
[2]*Department of Physics, Michigan Technological University, Houghton, Michigan 49931, USA*

(Received 12 August 2009; accepted 1 September 2009; published online 29 October 2009)

We report here, an investigation on electrical and structural-microstructural properties of an individual ZnO nanobelt via *in situ* transmission electron microscopy using an atomic force microscopy (AFM) system. The *I-V* characteristics of the ZnO nanobelt, just in contact with the AFM tip indicates the insulating behavior, however, it behaves like a semiconductor under applied stress. Analysis of the high resolution lattice images and the corresponding electron diffraction patterns shows that each ZnO nanobelt is a single crystalline, having wurtzite hexagonal structure ($a=0.324$ nm, $c=0.520\,66$ nm) with a general growth direction of $[10\bar{1}0]$. © *2009 American Institute of Physics*. [doi:10.1063/1.3241075]

Nanogenerators,[1] piezoelectric field effect transistors,[2] and piezoelectric diodes[3] were recently developed based on the unique coupling of piezoelectric and semiconducting properties of ZnO nanowires. The emergence of this nanopeizotronic area[4] requires further understanding on the electromechanical behavior of ZnO nanostructures. Although there were a few reports on the electromechanical behavior of ZnO nanowires,[5–8] no studies are devoted on the study of ZnO nanobelts, which are structurally different. Here, we present the study on the electrical and structural properties of an individual nanobelt via *in situ* high resolution transmission electron microscopy (TEM)-atomic force microscopy (AFM) system. All the measurements were carried out on a single tilt AFM-TEM holder (Nanofactory Instruments) in a JEM 4000FX TEM system that operated at 200 kV. Our ZnO samples were synthesized by thermal chemical vapor deposition method, as reported elsewhere.[9,10]

For *in situ* electrical measurement, an individual ZnO nanobelt was attached to the electromechanically etched tungsten tip by tungsten deposition using the focused ion beam (FIB) technique to ensure good electrical contact between the tip and the nanobelt. The different steps of the sample preparation are shown in Figs. 1(a)–1(c). In short, a nanobelt was picked up using the FIB probe [Figs. 1(a) and 1(b)] and attached on the tungsten tip [Fig. 1(c)] by the tungsten deposition. The tungsten tip with ZnO nanobelt was then transferred to the AFM-TEM specimen holder and approached to its opposite conducting AFM tip by the peizomanipulator. A schematic diagram of the experimental setup is shown in [Fig. 1(d)]. In order to clean the surface of the nanobelt and to achieve a good physical contact with the AFM tip, we applied a floating bias of 50 V to the nanobelt. Figures 2(a)–2(c) display the sequential images of a typical ZnO nanobelt undergoing to a stressed state by the gentle push of the peizodriven tungsten tip toward the AFM tip. It is to be noted that, for measuring the electromechanical properties in our experiments, nanobelts with shorter length of ~1–2 μm are chosen, to avoid bulking of the nanobelts. Figure 2(a) shows the bright field image of ZnO nanobelt just in contact with the AFM tip.

The current-voltage (*I-V*) characteristics of the ZnO nanobelt just in contact with the AFM tip [curve "a" in Fig. 2(d)] shows insulating behavior, probably due to less contact area and high contact resistance. By controlling the contacts of the nanobelt with the conducting AFM tip and also by bringing the nanobelt in a stressed state, it was possible to alter the *I-V* characteristics of the nanobelt. Figure 2(b) shows the ZnO nanobelt in a stressed state during the compression process and Fig. 2(c) shows the image at higher stressed state. A series of measured *I-V* curves with an increase of stress in ZnO nanobelt are respectively shown in Fig. 2(d). As we try to stress the nanobelt by delicate driving of the tungsten tip with the nanobelt against the AFM tip, a current of several nanoamps can be observed at a higher bias voltage (curve "b"). Although, the value of current obtained is not so high, however the nature of *I-V* curve indicates the

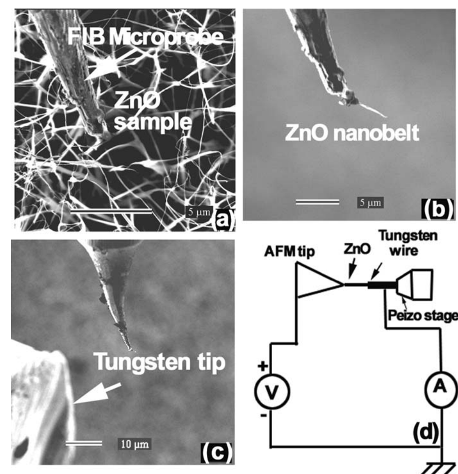

FIG. 1. Images from the FIB system showing (a) the as grown ZnO sample and the FIB probe, (b) a single nanobelt attached to the FIB probe, (c) the FIB probe with a nanobelt approaching the tip of the tungsten wire, and (d) Schematic of the current-voltage measurement setup.

a)Electronic addresses: aasthana@mtu.edu, ykyap@mtu.edu, and reza@mtu.edu.

0003-6951/2009/95(17)/172106/3/$25.00 © 2009 American Institute of Physics

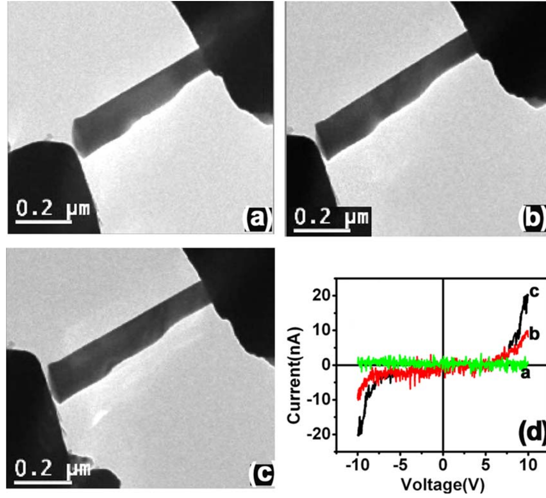

FIG. 2. (Color online) Bright field TEM images depicting the ZnO nanobelt (a) just in contact with the AFM tip; [(b) and (c)] under the applied stresses by compressing against the AFM tip. (d) A series of the representable *I-V* curves measured with applied stresses on the ZnO nanobelt. Curve "a" is for the ZnO nanobelt just in contact with the AFM tip, curve "b" and "c" are for the stressed states of the nanobelt.

semiconducting behavior of the nanobelt. With the increase in stress, the current is dramatically increased with start off voltage of 5.5 V bias [curve "c" in Fig. 2(d)]. In a large bias regime, the *I-V* curve can be differentiated to obtain a resistance R of the nanobelt ($R \sim dV/dI$,). We found that for this compressed state, the resistance of the nanobelt was decreased to 33 from ~80 MΩ in the lightly stressed state shown in Fig. 2(b).

The nonlinear *I-V* characteristics of these stressed states suggests for a semiconducting behavior. Thus our measurement system can be regarded as a metal-semiconductor-metal (*M-S-M*) circuit.[11] The related semiconducting parameters can be retrieved from the experimental *I-V* data in the bias regime >5 V, by the following relation,[12,13] $\ln I = \ln S + V\{[q/(k_B T)] - 1/E_0\} + \ln J_s$. Here S is the contact area associated with a bias, J_s is slowly varying function of the applied bias. The $\ln I$ versus V plot gives an approximately straight line with a slope of $[q/(k_B T)] - (1/E_0)$, and an intercept of $\ln S$. The representative $(\ln I)$-V curves are depicted in Figs. 3(a) and 3(b) corresponding to curve b and curve c in Fig. 2(d), respectively. Figure 3(c) shows the linear fits of curve b and c extrapolated to the $\ln I$ axis, showing nearly identical values of intercept. This means, $\ln S$ and the contact area (S) is merely identical for both of these stressed states. In the expression of $\ln I$, $E_0 = E_{00} \coth[E_{00}/(k_B T)]$, where $E_{00} = [(\hbar q)/2][n/(m^* \varepsilon)]^{1/2}$. Here, q is the elemental charge, k_B is the Boltzmann constant, m^* is an effective electron mass of ZnO nanobelt, and ε is the dielectric constant. We have estimated the specific sizes of the nanobelt from the bright field TEM image and thus the resistivity, ρ is obtained. The electron mobility, μ, is then calculated by using the relationship $\mu = 1/(nq\rho)$. For ZnO materials, $\varepsilon = 7.8\varepsilon_0$, ε_0 is the dielectric constant of a vacuum, and $m^* = 0.28 m_0$.[14] Based on this procedure, the resistance, resistivity, carrier concentration, and carrier mobility were extracted as summarized in Table I. As shown, nanobelt under the higher applied stress is having ~2.27-times higher charge carrier density but ~1.85-times lower charge mobility.

The structural properties of our nanobelts were also analyzed during the *in situ* TEM experiment. The general morphology shows that the ZnO nanobelts have an average width of ~150 nm and length of ~2 μm. A low magnification bright field image of a nanobelt and its corresponding electron diffraction pattern (in the inset) is shown in Fig. 4(a). The diffraction pattern suggests that our ZnO nanobelts are single crystals with wurtzite hexagonal structure ($a = 0.324$ nm, $c = 0.520\,66$ nm, $P6_3mc$), and a general growth direction of $[01\bar{1}0]$. The corresponding high resolution image, [Fig. 4(b)] taken from the rectangular region in Fig. 4(a) of the nanobelt also confirms these properties.

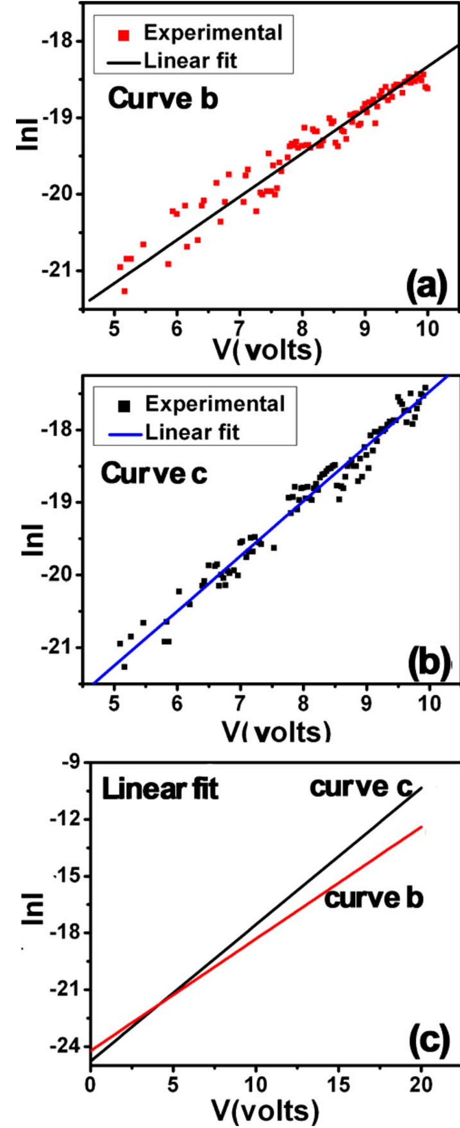

FIG. 3. (Color online) The ln *I-V* curves corresponding to (a) curve b and curve c in Fig. 2(d), respectively. (c) The linear fits of the curves in [(a) and (b)].

TABLE I. Electrical parameters of ZnO nanobelts.

Parameters	Curve b	Curve c
Resistance (MΩ)	80	33
Resistivity (Ω cm)	21.98	10.36
E_0 (meV)	25.9	26.4
Carrier concentration /(cm^3)	1.1×10^{17}	2.5×10^{17}
Mobility (cm^2/V s)	4.45	2.41

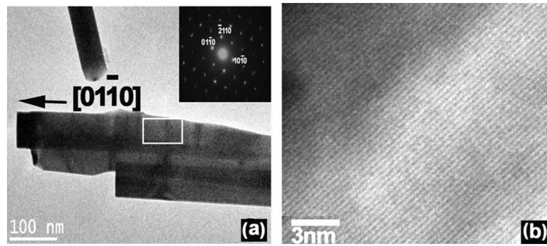

FIG. 4. (a) A ZnO nanobelt and its corresponding electron diffraction pattern (inset) and (b) the high-resolution lattice image.

Reported studies on the *in situ* electromechanical behavior of ZnO nanowires have shown that the electrical conductivity of ZnO nanowires decreased upon elastic bending.[5–8] However we found that the electrical conductivity of ZnO nanobelts is increased under applied stress. We explain our results as follows. Our ZnO nanobelts are short ($\sim$1–2 μm) as compared to these ZnO nanowires ($\sim$10–20 μm).[5,8] In our case, compression did not form physical bending on the nanobelt and thus did not produce the positively and negatively charged surfaces on the nanobelt as for the cases of ZnO nanowires. Hence, electrons are not trapped to decrease the electrical conductivity of the nanobelt when stressed as suggested for the case of bent ZnO nanowires.[2] Possible reasons for the increase in electrical conductivity of the stressed nanobelt under the present study could be (1) The generation of piezoelectricity in the stressed ZnO nanobelt. The applied compressive force causes charge separation along the stress axis. This charge separation induce an internal electric field inside the nanobelt and helps the electrons to move through the nanobelt. (2) The presence of dangling bonds at the surface of the ZnO nanobelts. These defects can have a dominant role in modulating its electrical conductivity.[15–17] Surface defects can produce surface states within the band gap making the ZnO nanobelt behaves like a weakly conductive metal. This allows the flow of conduction electrons near the surface region of the ZnO nanobelts as also reported by Lin *et al.*[7] As suggested from the data summarized in Table I, the mobility of the carrier concentration for the higher stressed nanobelt is decreased inspite of the appearance of piezoelectric effect, which should provide a driving force for the electrons to move faster. It is speculated that in the present case, the surface conduction mode started to dominate over the internal piezoelectric mode. The mobility of the charge carriers was decreased despite of the appearance of piezoelectricity. This means, the applied mechanical stress has the tendency to induce more surface defects. The detailed mechanism for this is unclear and is subjected for future study.

In conclusion, we have shown that the electrical transport properties of the nanobelt could be tuned from the insulating to semiconducting by inducing stress into the nanobelt using an *in situ* AFM-TEM stage. The semiconducting parameters were retrieved from the experimental *I-V* curves using the *M-S-M* model. The structural investigations of the nanobelts show that each nanobelt is single crystalline with hexagonal wurtize structure and grown in the $[01\bar{1}0]$ direction.

The authors acknowledge support from National Science Foundation (NSF-CMMI Grant No. 0926819 and NSF-DMR Grant No. 0820884).

[1]Z. L. Wang and J. H. Song, Science 312, 242 (2006).
[2]X. D. Wang, J. Zhou, J. H. Song, J. Liu, N. S. Xu, and Z. L. Wang, Nano Lett. 6, 2768 (2006).
[3]J. H. He, C. L. Hsin, J. Liu, L. J. Chen, and Z. L. Wang, Adv. Mater. (Weinheim, Ger.) 19, 781 (2007).
[4]Z. L. Wang, Adv. Mater. (Weinheim, Ger.) 19, 889 (2007).
[5]K. H. Liu, P. Gao, Z. Xu, X. D. Bai, and E. G. Wang, Appl. Phys. Lett. 92, 213105 (2008).
[6]Y. Liu, Z. Y. Zhang, Y. F. Hu, C. H. Jin, and L.-M. Peng J. Nanosci. Nanotechnol. 8, 1 (2007).
[7]X. Lin, X. B. He, T. Z. Yang, W. Gao, D. X. Shi, H.-J. Gao, D. D. D. Ma, S. T. Lee, F. Liu, and X. C. Xie, Appl. Phys. Lett. 89, 043103 (2006).
[8]P. M. F. J. Costa, D. Goldberg, G. Shen, M. Mitome, and Y. Bando, J. Mater. Sci. 43, 1460 (2008).
[9]S. L. Mensah, V. K. Kayastha, I. N. Ivanov, D. B. Geohegan, and Y. K. Yap, Appl. Phys. Lett. 90, 113108 (2007).
[10]S. L. Mensah, V. K. Kayastha, and Y. K. Yap, J. Phys. Chem. C 111, 16092 (2007).
[11]F. A. Padovani and R. Stratton, Solid-State Electron. 9, 695 (1966).
[12]Z. Y. Zhang, C. H. Jin, X. L. Liang, Q. Chen, and L.-M. Peng, Appl. Phys. Lett. 88, 073102 (2006).
[13]X. D. Bai, D. Goldberg, Y. Bando, C. Y. Zhi, C. C. Tang, M. Mitome, and K. Kurashima, Nano Lett. 7, 632 (2007).
[14]J. Hinze and K. Ellmer, J. Appl. Phys. 88, 2443 (2000).
[15]M. Huang, P. Rugheimer, M. G. Lagally, and F. Liu, Phys. Rev. B 72, 085450 (2005).
[16]Q. H. Li, Q. Wan, Y. X. Liang, and T. H. Wang, Appl. Phys. Lett. 84, 4556 (2004).
[17]M. S. Arnold, P. Avouris, Z. W. Pan, and Z. L. Wang, J. Phys. Chem. B 107, 659 (2003).